Journal of Nuclear Materials 466 (2015) 526–538

Contents lists available at ScienceDirect

Journal of Nuclear Materials

journal homepage: www.elsevier.com/locate/jnucmat

Review

Incorporating technetium in minerals and other solids: A review

Steven A. Luksic*, Brian J. Riley, Michael Schweiger, Pavel Hrma

Pacific Northwest National Laboratory, Richland, WA 99352, USA

ARTICLE INFO

Article history:
Received 21 May 2015
Received in revised form
27 August 2015
Accepted 28 August 2015
Available online 29 August 2015

Keywords:
Technetium
Immobilization
Waste form
Vitrification
Spinel
Sodalite
Rutile
Perovskite
Pyrochlore

ABSTRACT

Technetium (Tc) can be incorporated into a number of different solids including spinel, sodalite, rutile, tin dioxide, pyrochlore, perovskite, goethite, layered double hydroxides, cements, and alloys. Synthetic routes are possible for each of these phases, ranging from high-temperature ceramic sintering to ball-milling of constituent oxides. However, in practice, Tc has only been incorporated into solid materials by a limited number of the possible syntheses. A review of the diverse ways in which Tc-immobilizing materials can be made shows the wide range of options available. Special consideration is given to hypothetical application to the Hanford Tank Waste and Vitrification Plant, such as adding a Tc-bearing mineral to waste glass melter feed. A full survey of solid Tc waste forms, the common synthesis routes to those waste forms, and their potential for application to vitrification processes are presented. The use of tin dioxide or ferrite spinel precursors to reduce Tc(VII) out of solution and into a durable form are shown to be of especially high potential.

© 2015 Elsevier B.V. All rights reserved.

Contents

1. Introduction 527
2. Host phases for Tc incorporation 528
2.1. Spinel 528
2.1.1. High-temperature sintering 529
2.1.2. Aqueous precipitation and co-precipitation 529
2.1.3. Micro-emulsion synthesis 530
2.1.4. Sol-gel synthesis 530
2.1.5. High-temperature reflux 530
2.1.6. Hydrothermal syntheses 531
2.1.7. Liquid nitrogen-assisted synthesis 531
2.1.8. Ignition synthesis 531
2.1.9. Molten salt synthesis 531
2.1.10. Ball-mill-assisted synthesis 532
2.2. Sodalite 533
2.3. Rutile 533
2.4. Tin oxide 534
2.5. Pyrochlore 534
2.6. Perovskite 534
2.7. Goethite 535
2.8. Layered double hydroxides 535
2.9. Magnesium phosphates 536
2.10. Cementitous waste 536

* Corresponding author.
E-mail address: steven.luksic@pnnl.gov (S.A. Luksic).

http://dx.doi.org/10.1016/j.jnucmat.2015.08.052
0022-3115/© 2015 Elsevier B.V. All rights reserved.

2.11. Metal alloys 536
3. Summary 536
Acknowledgments 536
References 536

1. Introduction

Some 56 million gallons of waste were produced at the Hanford Site in Washington State as part of the production of plutonium during the last century. This waste currently resides in carbon steel tanks on the Hanford Site [1]. Technetium makes up 6% of the fission products from the use of uranium in the production reactors, and is thus a large part of the legacy waste that must be dealt with. Technetium is long-lived (half-life = 2.13×10^5 y) and environmentally mobile in its oxidized form (TcO_4^-) [2,3]. These properties add to the U.S. Department of Energy's urgency in immobilizing Hanford tank waste before leaking tanks become an environmental problem. Long-term immobilization of Tc is critical, as Tc is the dominant source of radioactivity in high-level wastes in the range of ten to hundreds of thousands of years [4] (see Fig. 1).

The current plan to treat the contents of Hanford tanks is to separate the wastes into a large-volume, low-activity waste (LAW) and a small-volume, high-level waste (HLW) fractions at the Hanford Tank Waste Treatment and Immobilization Plant (WTP), which currently is under construction at the Hanford Site. The LAW and HLW fractions will be vitrified in separate facilities within the WTP. Glass-forming additives and various components of the tank waste will be fed into waste-glass melters operating at temperatures of 1150 °C to vitrify the waste. One challenge to this approach is that Tc species, such as TcO_4^-, are volatile at temperatures below 900 °C [5,6], and this volatility is accentuated by the high temperatures found in vitrification melters. Volatiles from the melters, including Tc, will be captured in off-gas scrubbing systems that divert Tc, sulfur, and other waste-glass components to a dilute aqueous solution. The volatility of Tc makes it one of the more challenging elements to capture and store safely in glass.

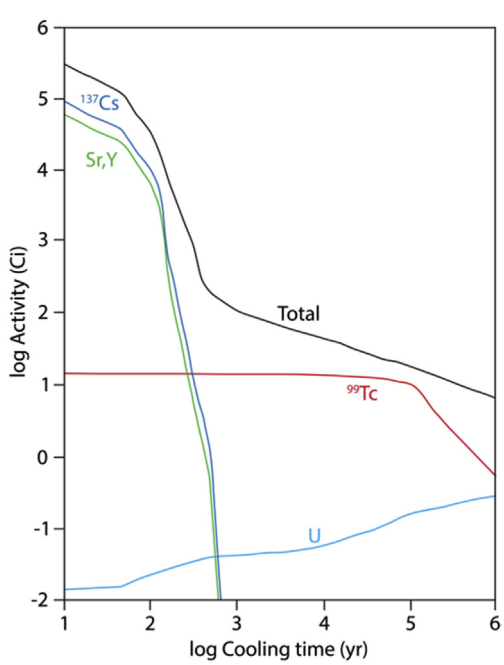

Fig. 1. Log/log plot of the activity (in Ci) of major radionuclides in high-level nuclear waste vs. time (in years) [4].

Alternatives to vitrification have been either proposed or are already underway for managing Tc wastes. In some places, Tc was simply released into the ocean [7]. Transmutation of metallic Tc into ruthenium has been attempted by the French with some success [8]. Other approaches include the formation of low-temperature waste forms for Tc-containing LAW such as cementitious waste forms [9–11], ceramicrete [10], and products of fluidized bed steam reforming [12].

Another approach to Tc immobilization is to remove the TcO_4^- from waste so it can be incorporated into a separate waste form. This can be achieved via ion exchange or with Tc-getters [13,14]. Qafoku et al. [15] recently investigated materials that could be used to remove TcO_4^- from solutions via reduction. The Tc then would be immobilized in a separate waste form such as Cast Stone [15].

The final approach discussed here is incorporation of Tc into a mineral lattice that would inhibit its volatility from the melter. If the Tc could be captured in a form that restrains volatility, such a material could transport the technetium into the bulk of the melt where it would be incorporated into the glass and where it would be less able to escape as a volatile gas during vitrification. If the TcO_4^- expected to be in the waste could be bound in a mineral structure, early experiments [16] show that this approach has the potential to increase Tc retention in the glass.

Technetium is present in nature in very small amounts as a result of natural uranium fission [17] and more recent human activities involving nuclear fission. Many different host mineral phases have been synthesized to include Tc in the mineral structure. These include spinel [18], sodalite [12], pyrochlore [19,20], perovskites [20], rutile [21], goethite [22,23], and layered double hydroxides [15,24,25]. Additionally, Tc-containing metal alloys have been studied as waste forms for immobilizing Tc [26,27].

The attributes of these mineral phases such as particle size, Tc loading, stability in waste melters, and hazards of reagents for synthesis are important when considering each mineral form. Large-sized mineral particles will present less surface area-to-volume and relatively high stability, thus limiting the interaction between the melt and any incorporated Tc. Thus, particle size over a micrometer is preferable to sizes of mere nanometers. High Tc loading in the mineral reduces the material volume added to the waste-glass melter. A host phase with low solubility in glass may delay decomposition of the phase, allowing less volatility than a more soluble phase. High-cost or hazardous synthetic routes for candidate materials are also undesirable factors that must be considered in selecting candidates.

To be useful for carrying Tc into glass melt, the phase chosen must be stable at very high temperatures and able to withstand the conditions of boiling glass feed. To be easily integrated into WTP operations, there must be a way that is energetically inexpensive and safe in terms of radiation exposure to synthesize the Tc-carrying material. Finding the suitable host mineral phase and how to synthesize it in an ideal form for maximizing the retention of Tc within the melter has not yet been accomplished. The goal of the present paper is to summarize the synthetic routes for materials that may serve as Tc waste-forms. This will include methods to

Table 1
Summary of mineral structures discussed in this review as well as chemical composition, space group, and theoretical Tc loading for each structure.

Mineral name	Mineral chemical formula	Space group	Theoretical Tc loading (mass%)	Demonstrated Tc loading (mass%)	Reference or related reference
Trevorite	$NiFe_2O_4$	*Fd3m*	4.4%	4.4%	[28,141]
Tc spinel	Mg_2TcO_4	*Fd3m*	36%	47%	[21]
Sodalite	$Na_8(AlSiO_4)_6(TcO_4)_2$	$P\bar{4}3n$	16%	1.1%	[12,29]
Rutile	$Ti_{0.6}Tc_{0.4}O_2$	$P4_2/mnm$	39%	39%	[21]
Tin dioxide	$Sn(Tc)O_2$	$P4_2/mnm$	3.1%	0.0079%	[30]
Pyrochlore	$Cd_2Tc_2O_7$	*Fd3m*	~37%	37%	[19]
Perovskite	$SrTcO_3$	*Pnma*	42%	42%	[4,21]
Goethite	FeO(OH)	*Pbnm*	unknown	0.5%	[23]
Layered double hydroxides	$Mg_6Al_2(OH)_{17}TcO_4$	*various*	15%	15%	[25]

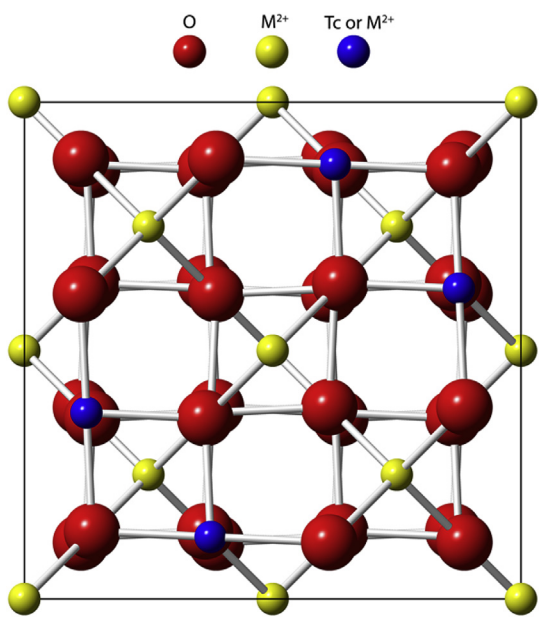

Fig. 2. Model of ulvöspinel unit cell of $Fe_2^{2+}TiO_4$ (where Ti can be Tc) after Muller et al. [21]. The structure is shown normal to the *a* direction.

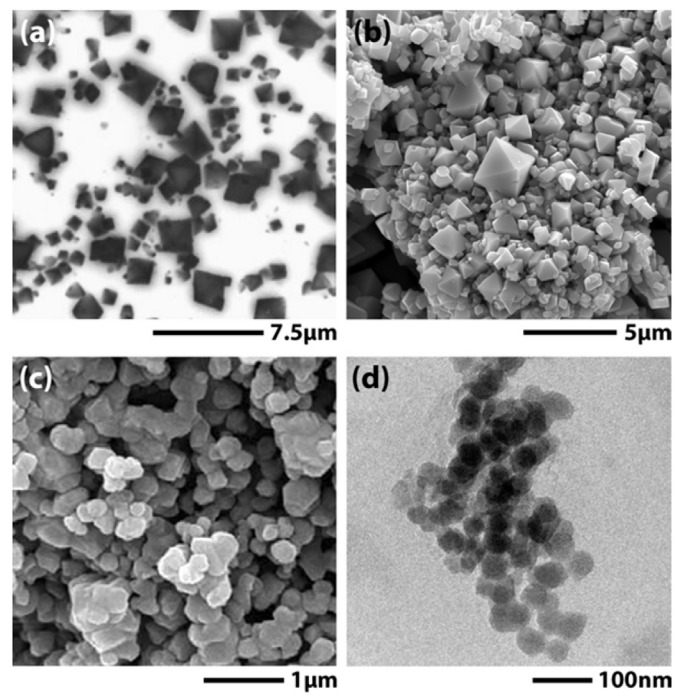

Fig. 3. SEM and TEM micrographs of spinel of various sizes including (a) large spinel made hydrothermally [46], (b) large spinel made with molten salt synthesis [47], (c) medium sized spinel made by aqueous precipitation [48], and (d) small spinel made with ball-milling [49].

make these various materials without Tc, as many of the mineral synthesis techniques found in the literature do not pertain to studies where Tc incorporation was a goal. Some consideration is given to which waste forms are most easily applicable to vitrification as a final fate.

2. Host phases for Tc incorporation

Table 1 lists crystal structures discussed in this section including the theoretical Tc loading in each structure [12,19,21,23,25,28–30]. Each mineral and the techniques that have been demonstrated to synthesize them are described below in greater detail.

The presumed Tc redox state in oxic environments, including the Hanford tank waste, is Tc^{7+} (TcO_4^-) [31], although non-pertechnetate species also are known to exist [32]. Some minerals, such as sodalite, can incorporate the Tc in the Tc^{7+} state [12,29]. Because many minerals can only incorporate the tetravalent ion Tc^{4+} [26], the Tc must undergo a reduction to be incorporated in them. The redox of Tc couples with another species within the proximity of the Tc^{7+}, such as divalent iron (Fe^{2+}) shown in Equation (1), could drive the reduction of Tc^{7+} to Tc^{4+} [22,28,33]. The Tc^{4+} ion has a radius of 78.5 pm, which is identical to high-spin Fe^{3+}, and very similar to Ti^{4+}, which has a radius of 74.5 pm [28]. Both Fe- and titanium-based minerals are therefore natural starting points in the search for a phase that can incorporate Tc^{4+} [28].

$$Tc^{7+} + 3e^- \rightarrow Tc^{4+} \quad (1a)$$

$$3Fe^{2+} \rightarrow 3e^- + 3Fe^{3+} \quad (1b)$$

2.1. Spinel

Spinel is a mineral of the cubic space group *Fd3m* that can coordinate a wide variety of metal cations in either tetrahedral (A sub-lattice) or octahedral (B sub-lattice) sites [34,35]. In all spinel, oxygen is arranged in a face-centered-cubic lattice, wherein these sites are situated. Two general types of spinel exist, normal spinel and inverse spinel. For a normal spinel, the general formula is $A^{2+}B_2^{3+}O_4$ where A^{2+} and B^{3+} are 2+ and 3+ metal cations that occupy the tetrahedral and octahedral sites, respectively. In an inverse spinel, the general formula is the same ($A^{2+}B_2^{3+}O_4$), but the 2+ cations occupy octahedral sites and 3+ cations are split between tetrahedral and octahedral sites. Common A^{2+} cations include Mg^{2+}, Ni^{2+}, Fe^{2+}, and Zn^{2+}, whereas the B^{3+} cations often include Al^{3+}, Fe^{3+}, and Cr^{3+}. Spinel containing tetravalent cations, such as

ulvöspinel, contain a 4+ metal cation instead of a 3+ cation and has the general formula of $A_2^{2+}B^{4+}O_4$. In this case, the 4+ cation is in the octahedral site and the 2+ cation is distributed between the octahedral and tetrahedral sites. A model of ulvö-type spine is shown in Fig. 2. Here, the most common B^{4+} cation in the literature is Ti^{4+} and divalent cations including Fe, magnesium, cobalt, manganese, nickel, and zinc (i.e., Fe^{2+}, Mg^{2+}, Co^{2+}, Mn^{2+}, Ni^{2+}, and Zn^{2+}) [34].

Magnetite, or Fe_3O_4 ($Fe^{2+}Fe_2^{3+}O_4$), is a type of inverse spinel often found in soil and sometimes proposed as a method to reduce pertechnetate to the less-mobile Tc^{4+} [36,37]. The short-lived ^{99m}Tc isotope has also been added to magnetite particles for use in medical imaging [38]. Magnetite is a special case of spinel because the Fe^{2+} often gets oxidized to Fe^{3+} in the melter, readily forming hematite [39,40]. While hematite has been predicted to be capable of including Tc^{4+} into its structure [41,42], magnetite is not a particularly durable phase in melter conditions, allowing the Tc it bears to be oxidized [16]. In contrast, spinel such as $NiFe_2O_4$ (trevorite, $Ni^{2+}Fe_2^{3+}O_4$) or gamma-Fe_2O_3 (maghemite) can be much less redox sensitive because the only Fe^{2+} present will be from that needed to charge balance the Tc^{4+} introduced in the system, and the Fe^{3+} is not likely to undergo reduction at melter operating temperatures.

While many methods exist to make spinel, synthesis of Tc-bearing spinel is dominated by high-temperature methods first employed by Muller et al. [21]. Most research into Tc mixed oxides (spinel, pyrochlore, perovskite, rutile, etc.) has used high-temperature sintering to produce test materials [18,21,43,44]. Many papers describe a host of alternative routes to spinel; however, only a few have been demonstrated for making Tc spinel [28,45].

Fig. 3 shows scanning electron microscopy (SEM) and transmission electron microscopy (TEM) micrographs of spinel without Tc at various different sizes made by different synthesis techniques presented in the literature [46–49].

2.1.1. High-temperature sintering

Muller et al. [21] described many new forms of Tc-containing spinel, all achieved by heating oxides to circa 1200 °C. High-temperature syntheses of several phases were described and provided a foundation for subsequent Tc-mineral studies. The approach they used involved finely mixed oxides sintered under inert atmosphere in sealed platinum vessels at temperatures at or just above 1200 °C. Grinding the starting oxides in acetone or mixing with 20 mol% of 2NaCl:NaF used as a mineralizer increases the reactivity of oxides [50]. This method has been used with very little variation to study Tc-bearing phases [18,21,43,44].

The high-temperature sintering has been shown to produce pure, micrometer-sized Tc-bearing spinel of varied stoichiometry [21]. However, the challenges of high-temperature synthesis include engineering demands and the need to first reduce Tc from Tc^{7+} to Tc^{4+}. Energy is needed to heat the samples, oxygen pressure must be controlled, and volatile Tc poses a risk if containment is compromised while at high temperature. The process also requires TcO_2 as a reagent, which would have to be isolated and reduced from waste streams as a prerequisite to WTP application. This makes the synthesis a multi-step process and more imposing on the existing WTP flow sheet than a system that could incorporate the Tc directly from the waste stream.

The spinel forms described in the work by Muller et al. [21] included A_2TcO_4 spinel, where A = Mg, Co, Mn, Zn, Ni, and/or Cd [21]. Pure products were reported in all cases except for Co_2TcO_4, $CoNiTcO_4$, and $NiCdTcO_4$, where impurities were detected with X-ray diffraction (XRD). Most of these have Ti-based analogues and many have been demonstrated as mixtures of Tc and Ti. Solid solutions of Tc–Ti spinel have been demonstrated including a series of Ti-Tc-Mg spinel with both end members (i.e., Mg_2TcO_4 and Mg_2TiO_4) [18,43,51]. Lattice parameters increase with the increasing degree of Tc substitution, and these data agreed with parameters for Mg_2TiO_4 and Mg_2TcO_4 set forth by Muller et al. [21]. It is noted that the syntheses of Tc phases occur at lower temperatures than the Ti analogues; this is thought to be due to the fluxing action of vaporous Tc at these temperatures, compared to the much lower vapor pressure of Ti.

Unsuccessful syntheses also were reported, including Cu_2TcO_4, Ni_2TcO_4, $NiTc_2O_4$, Fe_2TcO_4, $FeTc_2O_4$, and Zn_2TcO_4 [21]. These were described as having little or no reaction at high temperatures, or breaches in the Pt foil at long reaction times, thus preventing synthesis. For a successful synthesis, the metal cations must be suited for the octahedral and tetrahedral sites in the structure. The Tc^{4+} ion has a strong preference for the octahedral site, so a divalent cation then needs to fill half of the octahedral sites and the part of the tetrahedral sites as well. To this end, a cation, such as Mg or Mn, with no particular affinity for either tetrahedral or octahedral sites should be chosen. This is the explanation given as to why the Ni_2TcO_4 end-member (Ni having a preference for octahedral sites) and Zn_2TcO_4 end members (Zn having a tetrahedral preference) do not form by themselves, but a $NiZnTcO_4$ will form readily [21].

Increasing the Tc loading of titanate spinel may be possible through a process that incorporates oxides into spinel lattices. Titanate spinel of the form Zn_2TiO_4 can be sintered with TiO_2 to create a solid solution of up to a TiO_2:Zn_2TiO_4 ratio of 0.28 [52]. This creates a single-phase product that has increased occupancy of Ti^{4+} into octahedral sites and Zn^{2+} vacancies in tetrahedral sites. The TiO_2 is introduced as rutile and sintered at 950 °C for this process. The TcO_2 oxide possibly could combine with Zn_2TiO_4 spinel via an analogous method [53].

Sintering oxides at pressures of GPa has been shown to create $MgFe_2O_4$ spinel with up to 0.35 mass% rhenium, [54]. Rhenium is a non-radioactive chemical surrogate for Tc, with similar volatility and chemical speciation [6,36].This is meant to mimic the geological conditions that yield Re-bearing spinel, with concentrations on the order of fractions of ~1 ng Re/g of spinel [55].

2.1.2. Aqueous precipitation and co-precipitation

Co-precipitation is a two-step reaction in which dissolved cations are mineralized into nuclei, where particle growth then occurs [40]. The basic procedural template involves combining divalent and trivalent metal salts in solution, and mineralizing with a strong base. The reaction is generally given in Equation (2) where $x >> 8$ and M represents a divalent cation (e.g., Ni^{2+} or Fe^{2+}) [56].

$$(x \geq 8) \quad MCl_2 + 2FeCl_3 + xNaOH \rightarrow MFe_2O_4 + (x-8)NaOH + 4H_2O + 8NaCl \tag{2}$$

Lukens et al. [28] demonstrated Tc incorporation into spinel with an aqueous precipitation method. This method is performed at much lower temperatures than the procedure described by Muller et al. [21] (90 °C instead of 1200 °C), and yields smaller product size (nanometer-sized instead of micrometer-sized) with lower Tc loading (4 mass% instead of 40 mass%). The starting form of Tc is TcO_4^- instead of TcO_2, and a ferrite spinel is formed instead of titanate. Starting the reaction with an aqueous TcO_4^- ion is more congruent with the aqueous conditions of Hanford waste. Ti^{4+} incorporation into magnetite, which has been well characterized, suggests that Tc^{4+} may likewise incorporate into magnetite, given that Ti^{4+} and Tc^{4+} are similar in radius (0.745 and 0.785 Å, respectively) [37]. The lower reaction temperature reduces the process energy cost and removes concern for Tc volatility.

In the method by Lukens et al. [28], salts of Fe^{2+} and Fe^{3+}, an additional divalent metal (Ni^{2+}, Mn^{2+}, Mg^{2+}, or Co^{2+}), and TcO_4^- are dissolved in anoxic water. Then, NaOH is added to increase the pH and precipitate the metal ions. In this case, the reduction of Tc^{7+} to Tc^{4+} is driven by the oxidation of Fe^{2+} to Fe^{3+} through the redox couple presented above in Equation (1). The results of this process showed that 99 mass% of Tc is removed from solution by these methods, with spinel as the major product [28].

Analysis of spinel products by both methods used by Lukens et al. [28] shows crystal sizes ranging from 19 to 38 nm for the so-called oxidation method (mineralization in the presence of nitrate), and 9–24 nm for the so-called co-precipitation method (mineralization without nitrate). Extended X-ray absorption fine structure analysis was used to examine the ordering of Tc in the structure, and showed high Tc clustering for the magnetite and ferrites other than $Tc_{0.1}Ni_{1.1}Fe_{1.8}O_4$ (trevorite). This high clustering suggests that a separate Tc phase could be occurring in cases other than for trevorite.

To date, the method from Lukens et al. [28] is the only aqueous precipitation approach to produce Tc-bearing pure trevorite spinel. However, other methods are described here for making spinel from solution, and most do not include Tc. Many of these methods involve precipitating intimate mixtures of oxides or other spinel precursors, followed by sintering to crystalize the product. Other procedures produced spinel directly, without further heating. A discussion of these procedures follows in Section 2.1.3.

Tc-bearing magnetite is co-precipitated from a solution with pH ranging from 12.5 to 13.1 when Fe^{2+} cations (from $FeCl_2$) and TcO_4^- (from NH_4TcO_4) are added in the presence of ferrihydrite [36]. The Fe^{2+} deposits on the ferrihydrite nano-particles at high pH and reduces the Tc^{7+} to Tc^{4+} as a result of heterogeneous surface-catalyzed reduction, which fills octahedral sites as the formation of magnetite occurs and particles grow. A Tc content of ~500 ppm in magnetite was achieved from a starting solution of ~30 μM NH_4TcO_4. While Tc was totally removed from solution by this method, 20–60% was released back into solution when exposed to oxidative conditions. This leaching was found to remove Tc from an outer layer of the magnetite nano-particles, which was oxidized into goethite. Leaching was apparently arrested after the initial goethite-forming oxidation, even after several months under oxidative conditions [36].

Unfortunately for our purposes, nanometer-sized particles have received most of the attention in the literature because of interest in their use in batteries and conductors. Small particle sizes allow for easier diffusion of Tc from the lattice, re-oxidation, and Tc release [57]. To some extent, nano-particles can be armored with an amorphous silica layer, that may mitigate Tc diffusion by coating nano-particles during a second precipitation step after the initial particles form [58].

Salts used for precipitation of spinel without Tc including nitrates [59], sulfates [60], and organic ligands [40,50]. Commonly used bases include NaOH [56], KOH [60], and NH_4OH [61]. Divalent metal salts can include Zn^{2+} [62], Mn^{2+} [56], Co^{2+} [63], Fe^{2+} [64], and Ni^{2+} [65], although others have been demonstrated. Co-precipitation and subsequent heat treatment can produce micrometer-sized spinel several hundred degrees lower than the simple sintering of oxides [66].

In cases of redox sensitivity, such as the synthesis of magnetite, anoxic water must be used to prevent over-oxidation due to O_2. One study achieved a pure product without the need to control atmosphere, using ambient O_2 as an oxidizing agent and adjusting starting concentrations of Fe^{2+} and Fe^{3+} [64].

In the case of magnetite synthesis, NH_4OH was found to be superior to alkali hydroxides, where a cation concentration of 0.1 M, a temperature of 45 °C, and mixing of the cation solution into the basic solution was found to be ideal [60,61,67].

Many products require sintering to 300–900 °C to promote crystallinity, but aging with urea at 90 °C or heating in boiling water for several hours can yield nanometer-sized products without further sintering [56,62].

2.1.3. Micro-emulsion synthesis

Micro-emulsion is a form of co-precipitation in which particle growth is inhibited because the reacting solution is contained in discrete bubbles within an organic liquid. This is a common technique and is used to limit the amount of reagents that can interact, thereby limiting the potential particle size. While limiting particle size is not an aim of synthesizing a Tc host phase, much of the literature is dedicated to creating nanometer-sized particles. Furthermore, most emulsion methods often require sintering of the product to promote crystallinity [50,58,59,68–70], which the method by Lukens et al. [28] avoids.

A survey by Calbo et al. [50] of unconventional trevorite syntheses compares micro-emulsion to other methods, showing that it produces more crystalline product at lower temperatures than conventional sintering, but its performance is inferior to co-precipitation. In a typical technique, an aqueous solution of $NiCl_2$ and $FeCl_3$ is mixed in a 1:5 M ratio with isooctane and two surfactants, and treated ultrasonically. A second micro-emulsion of ammonia is then prepared, and mixed with the first emulsion. After an hour of ultrasonic mixing, a product layer can be isolated, dried, and fired at 800 or 1000 °C [50]. Ricin oil and NaOH [68] or methylamine [70] can be used in place of octane and ammonia, and organics such as cyclohexane [69] or toluene [59] in water also can be used to create an emulsion. Particle size is often less than 10 nm.

2.1.4. Sol-gel synthesis

While co-precipitation nucleates spinel in solution, other aqueous methods can tend to precipitate an amorphous product that can be calcined into spinel, albeit at lower temperatures than would be necessary with conventional sintering. Sol–gel processes condense precursor materials in a 'gel' through polycondensation reactions that form a network of nanometer-sized particles when calcined. The sol–gel method allows the precursors to be intimately mixed and crystallize into spinel at a lower temperature. Spinel synthesized using such a scheme yield 5–150 nanometer-sized particles.

Synthesis of spinel by a sol–gel method can be done with various metal salts and solvents. Nickel and ferric nitrates in a gel of ethylene glycol are used to synthesize trevorite [71]. Acetonates of nickel and iron also can be dissolved in ethanol, then combines with nitric acid and acetylacetone to the same effect [50]. Nitrates of metals in aloe vera extract have even been shown to create a sol [48]. All three of these approaches require sintering of products after the sol is dried. Particle size of the product depended strongly on the sintering temperature [72]. While this method does operate at lower temperatures than those described by Muller et al. [21], heating is required to produce crystallized 5–150 nm-sized spinel. This process remains untested in regards to Tc compatibility.

2.1.5. High-temperature reflux

Another approach to spinel synthesis is refluxing organometallic reagents in liquids with high boiling points. During reflux, a solvent is heated in a vessel near its boiling point and allowed to continuously condense and flow back into the vessel. Synthesizing nanometer-sized spinel crystals in a high-temperature reflux over 100 °C takes advantage of the heat refluxing the solvent and the relative instability of the metal complexes as compared to the spinel form.

Various related methods are described in the literature. Cobalt

and iron acetates have been reacted at 260 °C to reflux in phenyl ether and hexadecanediol for 30 min, and then precipitated spinel when ethanol was added [73–75]. Alternately, metal acetylacetonates can be thermally decomposed in olymine at 220 °C [76]. In a series of papers, Song et al. [73–75] described a seed-mediated growth that used smaller products of the refluxing as a seed for crystal growth in a subsequent round of reactions. In a seed-mediated reaction, 12-nm crystals were grown from 4-nm precursors. The third report (Song et al. [75]) describes using seeds of one composition with a reflux batch of another composition to create core–shell nano-particles, such as 6-nm $CoFe_2O_4$ crystals with a 1-nm shell of $MnFe_2O_4$ [75]. Seeding also was shown to increase crystallinity for several other precursor-preparation methods, besides high-temperature reflux [77].

2.1.6. Hydrothermal syntheses

Hydrothermal methods use sealed pressure vessels to obtain above-boiling temperatures and pressures for aqueous reactions [71]. If an increase in either pressure or temperature leads to an increase in grain growth, particle sizes can be increased. Hydrothermal syntheses methods account for the largest spinel achieved by aqueous methods (larger than 1 μm) [46]. No literature examined hydrothermal methods with Tc chemistry, but extant aqueous methods with Tc may be adapted to hydrothermal synthesis.

In a straight-forward method, $CoCl_2$ and $FeCl_3$ were reacted in 2 M NaOH solution. Next, hydrothermal treatment was performed at 130 °C [78]. Alternately, iron citrate and zinc and manganese acetates are dissolved in a 50% NH_3 solution and autoclaved to over 130 °C [79]. While these methods produced spinel that were only tens of nanometers in size, larger sizes are possible. For example, in a hydrothermally assisted micro-emulsion, $Ni(NO_3)_2$ and $Fe(NO_3)_3$ nitrates, polyoxyethylene(10)nonylphenyl ether, and hexane can be added together, followed by addition of cetyltrimethylammonium bromide, iso-amyl alcohol, and urea and an autoclave heat treatment for 30 h, producing 100-nm crystals [80]. Additionally, 200-nm crystals were synthesized when $Zn(OAc)_2$ and $FeSO_4$ were dissolved in water with stirring, hydrazine was added, and the solution was autoclaved at 180 °C for 14 h [81]. Various other starting materials have included $Ni(OH)_2$, FeO(OH) (goethite), and Fe_2O_3 autoclaved in the presence of NaCl. Use of different reagents demonstrated that different morphologies of products can be produced, with goethite proving more reactive and producing more crystalline products than Fe_2O_3 [82]. The largest sized spinel product was obtained from goethite and amorphous NiO from a $Ni(NO_3)_2$ precipitation, which was hydrothermally treated at 180–200 °C with 2 M NaOH [46]. These achieve sizes of >1 μm for single crystals—a notably large size for trevorite produced from aqueous synthesis. Goethite and amorphous NiO, which are less thermodynamically stable than well crystalline oxides, were intended to be more reactive phases than Fe_2O_3 or well-crystallized NiO. This is thought to be a contributor to the large particle sizes obtained in that study.

Kuznetsova et al. [78] examined the effects of ultrasonic treatment of solutions before heating with and without a microwave heat source. Microwave heating led to product in less time than conventional heating, and ultrasonic pre-treatment increased the performance of microwave heating even more. These experiments also showed that ultrasonic treatment was only effective if it preceded hydrothermal heating by <2 h. These effects may be useful for increasing the kinetics of methods that show promise, such as the Chen [46] method.

2.1.7. Liquid nitrogen-assisted synthesis

In what must be considered a unique approach, Jang achieved 100-nm sized particles of $CoMn_2O_4$ below room temperature [63]. By promoting the autoxidation of Mn_3O_4 from $Mn(NO_3)_3$ and $Mn(OH)_2$, the reaction proceeded from the addition of dilute $Co(NO_3)_2$ and $Mn(NO_3)_3$ to LiOH at pH 11. The solution was stirred in air for 12 h before being rinsed, atomized into liquid nitrogen, and freeze-dried. A nearly pure 100-nm-sized product of $(Co_{0.75}Mn_{0.25})_3O_4$ was obtained. The same reaction yielded spinel when carried out with only $Mn(NO_3)_3$ in the absence of Co, but not with $Co(NO_3)_2$ in the absence of Mn, which only formed Co^{2+} and Co^{3+} hydroxides. The low-temperature atomization and control of Mn^{2+}/Mn^{3+} redox is what allowed for spinel formation. Because Fe also forms divalent and trivalent ions, ferrites might be produced by a similar reaction using Fe instead of Mn. This could possibly lead to another low-temperature method to make Tc-bearing phases like trevorite.

2.1.8. Ignition synthesis

Alarifi et al. [83] reported the synthesis of trevorite by combining $Ni(NO_3)_2$ and $Fe(NO_3)_3$ with glycine, which was heated to ignition. The chemicals were mixed in a porcelain crucible, which was heated until a fluffy black powder was formed from a sudden onset of sparks. The particles formed are approximately 4–67 nm. Because Tc is easily oxidized to Tc^{7+} in air, it would likely not incorporate into the spinel lattice under these conditions, making ignition unlikely to be useful for Tc incorporation, but was included here for completeness.

2.1.9. Molten salt synthesis

Molten salt synthesis is a well-known industrial process that makes use of a liquid salt flux to dissolve oxides at low temperatures [84]. When using liquid salt, the mobility of oxides is increased compared to high-temperature sintering, and reactions similar to high-temperature sintering can occur faster and at lower temperatures [85]. Factors such as the basicity of the salt melt, the temperature, and the speciation of the reagents can all affect the product composition, size, and reaction kinetics [86]. Compared with high-temperature sintering, the molten salt synthesis technique generally provides a more homogeneous product (as material transport in the reaction is increased), decreased agglomerations (as the salt flux coats the particles and inhibits necking), and at lower reaction temperatures (as much as ≤500 °C) [84]. It is a flexible technique, but has never been successfully adapted for Tc-spinel synthesis.

In a typical synthesis, NiO and Fe_2O_3 are combined with NaCl and KCl [85]. Spinel forms and precipitates out of the salt flux upon heating to 900 °C for 0.5–3 h. Particle sizes resulting from this type of experiment are generally on the order of 0.1–10 μm [87]. When LiCl and KCl are used as a low-melting flux, the lowest temperature needed for near–complete reaction of NiO and Fe_2O_3 into trevorite is 350 °C, [88]. This flux was heated to several temperatures and held for up to 6 months to achieve reaction. All treatments at <1000 °C yielded some unreacted oxides.

Salts can be used instead of oxides. For example, $Ni(SO_4)$ and $Fe(NO_3)_3$ were mixed with NaOH and NaCl and heated to 700 °C [89]. The salt component and intimate combination of reagents through mixing allowed the resultant spinel to form at slightly lower temperatures than would be the case for mixing of larger grain oxides. After firing at 700 °C for 1 h, the resulting spinel grew to ~10 nm, which was unusually small for molten salt synthesis.

Template growth is one approach for molten salt synthesis in which a less-soluble, specifically shaped reactant is coated and reacted with a more soluble reactant [90]. This is demonstrated in several ways with molten salt synthesis and a tailored product shape can be created if less soluble reactants can be used. Preferred growth of crystal facets also is possible because the augmented mobility of reactants allows for selective placement of

precipitating material onto energetically favorable edges. Using this approach, rod-shaped $NiFe_2O_4$ was prepared from molten chlorides by Hayashi, starting from acicular Fe_2O_3 [91]. Also, hexagonal plates of NiO crystals can be made and used in template growth [92]. Template-growth molten salt synthesis using this phase of NiO as a reagent could provide an energetically favorable and easily characterized $NiFe_2O_4$ product. If this type of spinel were added to a waste glass melt, the distinct hexagonal shape of the thus-formed spinel would be helpful in showing signs of reaction in a glass melt, as it would be distinguishable from in-grown octahedrally shaped spinel.

Even when salt fluxes are minor components, they can play a role in promoting ordering of oxides into spinel. In the study of trevorite syntheses by Calbo et al. [50], products were sintered both with and without the presence of 20 NaCl:NaF. The presence of the salt did reduce impurities in one of the final sintered products [50].

In work by the current authors [47], ReO_2, K_2ReCl_6, and TcO_2 were added to vacuum-sealed ampoules of Fe_2O_3, NiO_2, and chloride salts. After heating to 900 °C, Re^{4+} was shown to have oxidized to ReO_3, and the Tc formed a non-spinel complex with Fe^{2+}, likely bound to the surface of the trevorite that did form.

2.1.10. Ball-mill-assisted synthesis

Because both heat and redox chemistry are complications for syntheses involving the volatile and easily oxidized Tc, a method without either heat or redox active reagent requirements is attractive. Ball-milling fits this description as starting materials, chiefly oxides, are homogenized and smashed in a ball mill for several hours, eventually leading to agglomerations of pure spinel product. Separated and reduced Tc would be required for this synthesis. The dispersal hazards of fine-grained oxides being violently impacted by milling media is unique to this method, and would require special consideration for Tc.

In one example, Fe_2O_3 powders coupled with either NiO or ZnO were milled at 10G acceleration with steel or corundum media to synthesize spinel nano-particles [93,94]. The reaction was complete at 35 h. The internal temperature of the mill reached 150 °C, due to the mechanical energy. Based on XRD peak widths, the crystallite size was estimated to be 6-nm. When corundum was used as the milling media, it was detected by XRD in the product. Similar results were reported when a planetary mill was used to

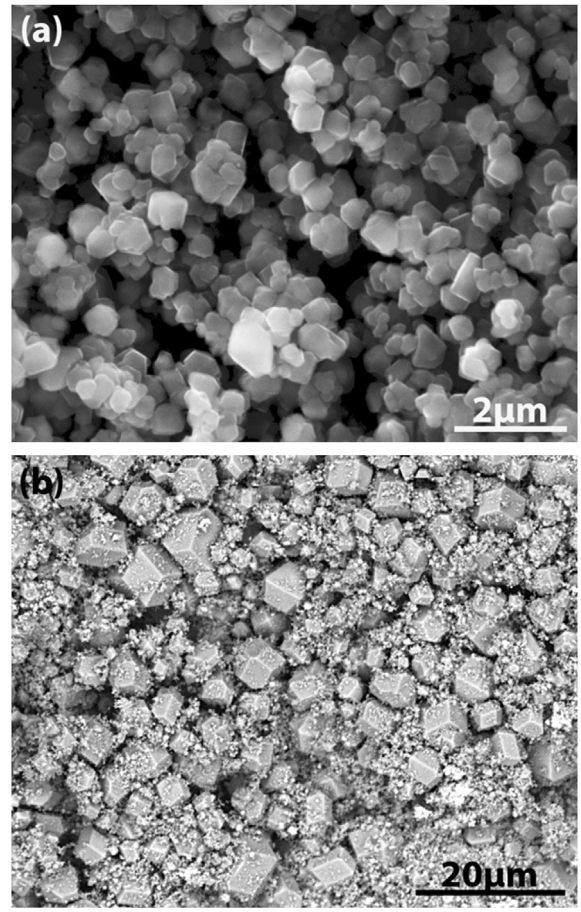

Fig. 5. SEM micrographs of (a) Tc-sodalite [12] and (b) Re-sodalite [16].

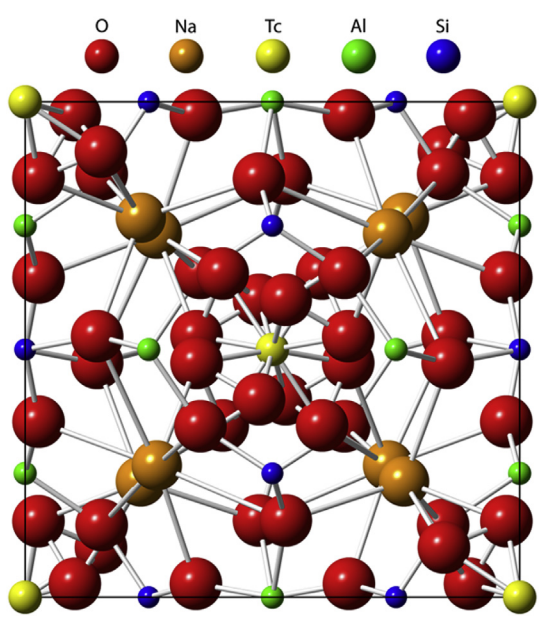

Fig. 4. Theoretical model of Tc-containing sodalite unit cell of the formula $Na_8(AlSiO_4)_6(TcO_4)_2$ after the perrhenate sodalite by Mattigod et al. [29]. The structure is shown normal to the *a* direction.

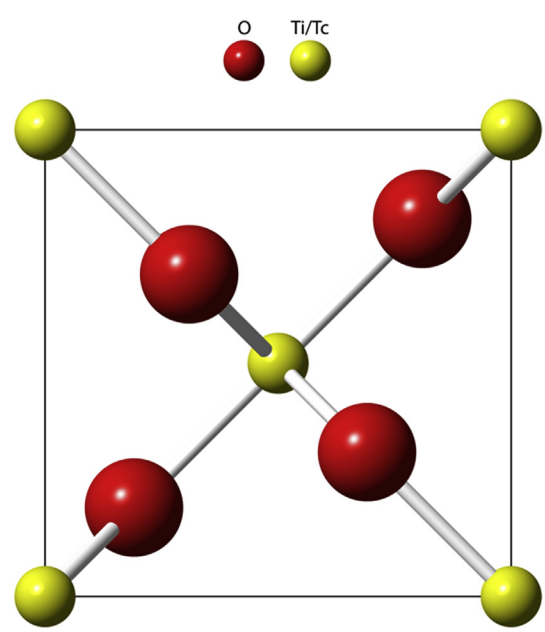

Fig. 6. Model of Tc replacing Ti in rutile (TiO_2) unit cell. The structure, from Henderson et al. [142], is shown normal to the *c* direction.

combine NiO and Fe_2O_3; the rate of formation of spinel decreased after 11 h of ball-milling, and resulted in 5-nm spinel [49].

In another example, low-energy milling completed formation $MgAl_2O_4$ after 160 h [95]. Domanski et al. [95] compared Al_2O_3, γ-Al_2O_3 (transition alumina), and AlO(OH) and found that the γ-Al_2O_3 was much more reactive than either of the two other sources. Taking advantage of more reactive phases of reagents to boost product crystallinity in this study is comparable to the positive results seen in Chen et al. [46], and again highlights the usefulness of more reactive reagents in producing higher purity products in less time. On a related note, short-term, low-energy milling required subsequent heating to 1000 °C to observe formations of $MgAl_2O_4$ [96]. In this work, grinding was done in corundum media at 600 revolutions per minute, yielding significant corundum contamination after 110 min.

2.2. Sodalite

Sodalite is a crystal of the cubic space group $P\overline{4}3n$ composed of 4- and 6-membered rings with the general formula of $A^{I}_{8}(B^{III}C^{IV}O_4)_6D_n$, where A^+, B^{3+}, and C^{4+} are generally 1+ (and sometimes 2+), 3+, and 4 + cations and D can be n moles of a variety of different 1- (e.g., Cl^-, OH^-, ReO_4^-, TcO_4^-; $n = 2$) [12,29,97–100] or 2- (SO_4^{2-}; $n = 1$) [101] anions or H_2O [102]. The structure of the TcO_4^--containing sodalite is presented in Fig. 4. Because sodalite can be formulated to contain either TcO_4^- or its analogue of ReO_4^-, this makes study of this mineral in non-radioactive scenarios a possibility. A wide range of methods can be used to synthesize sodalite; however, the one demonstrated for making sodalite with the TcO_4^- [12] and ReO_4^- [29,99] oxyanions is a low-temperature hydrothermal method [12,29].

In efforts to characterize steam bed reformers, TcO_4^-- and ReO_4^--bearing sodalite was synthesized by Missimer et al. [12] (Fig. 5a). They combined 6 g of $NaReO_4$ with 0.6 g of zeolite 4A, water, and NaOH in a pressure vessel and heated the mixture to 225 °C for 7 days, at which time approximately 1.5 g of perrhenate sodalite was collected by filtration. For pertechnetate sodalite, ~0.33 g of $NaReO_4$ was replaced with $NaTcO_4$, and the heat treatment was extended to 8 days. The structures and presence of Tc in the pertechnetate sodalite were confirmed by XRD and EDS, respectively. The Tc-loaded sodalite contained Re and Tc, but elemental analysis was not done to determine an exact ratio.

Mattigod et al. [29] produced ReO_4^--sodalite through hydrothermal processing at 175 °C for 1 day (Fig. 5b). Dickson et al. report making a perrhenate/nitrate [99] sodalite by combining $NaReO_4$ with zeolite A and NaOH and heating to 90 °C. Their XRD analysis appeared to show the Re product was pure.

2.3. Rutile

Rutile is of the tetragonal space group $P4/mnm$ and is nominally an allotrope of TiO_2. The structure of this mineral is shown in Fig. 6 with a theoretical replacement of Ti with Tc. This crystal structure can incorporate diverse formulae of Ti, V, Nb, Ta, Mo, Re, and other metals [103]. Rutile is a fairly inert structure that may prove a useful candidate host phase for Tc. Rutile is compositionally TiO_2, and has been shown to incorporate Tc in high-temperature syntheses [21].

Muller et al. [21] first showed that TcO_2 could be sintered with anatase TiO_2 to form a Tc-rutile. Anatase transitions to rutile when heated, and TcO_2 will join the rutile structure if present. This was done in the same manner as the other high-temperature syntheses by mixing oxides in Pt crucibles and heating to >1000 °C. A more recent study [104] reported on the synthesis of $Tc_{0.1}Ti_{0.9}O_2$, with Tc starting as NH_4TcO_4, and mixed with TiO_2 (anatase) powder. While samples sintered to 1300 °C in flowing argon successfully incorporated Tc into the rutile phase, Tc reduction to metal was seen at higher temperature. Off-gassing of O_2 from Tc reduction caused fissuring of the samples and a Tc-deficient layer in the sample. Stewart et al. [104] noted that the loss from rutile is greater than from Tc-perovskite phase exposed to the same heating conditions, and suggested that migration of Tc in the perovskite phase is inhibited compared to that of the rutile phase.

Full conversion of anatase-to-rutile within 1 h is achieved at 120 °C lower when porous, nanometer-sized particles, a mildly reducing atmosphere, and additives such as Fe_2O_3 are used. This indicates that it is possible to lower the incorporation temperature of Tc into rutile from what had been originally reported by Muller et al. [21]. Particle size can be modified with additions to sintering reagents. In particular, the addition of 1 mol% of Fe_2O_3 or MoO_3 increased the grain size of rutile formed at 800 °C fivefold, to >2 μm [105]. The addition of Fe_2O_3 is shown to catalyze the anatase-to-rutile transition [106], which is the reaction demonstrated by Muller et al. [21] to incorporate Tc into rutile. Reducing atmospheres and electrical fields also increase reaction rates and particle sizes [107–110].

Preparation of porous, nanometer-sized anatase particles can be accomplished by the sol–gel method of polyalkylene oxide and tetrabutyl orthotitanate. Precipitating this product with other oxides would create a more intimate mixture of anatase and any additives deemed necessary to promote the anatase-to-rutile conversions [111]. This method would be a promising route for preparing readily reactive anatase mixtures, and lower temperature rutile-forming methods.

Rutile and other phases can be formed by self-propagating, high-temperature synthesis [112,113]. Highly reactive redox pairs such as metallic Ti or Zr and oxides such as MoO_3, Fe_2O_3, or Tc_2O_7 are combined and ignited, creating a multiphase product. The metals act as redox couples and exchange oxidation states in extremely quick and exothermic reactions, yielding pyrochlore, perovskite, rutile, or even alloys. The redox of the reaction and the extent of oxidation of the final products can be controlled by the ratio of starting materials. Molybdenum was used by Laverov et al. [114] as a surrogate for Tc, and rutile phases formed by self-

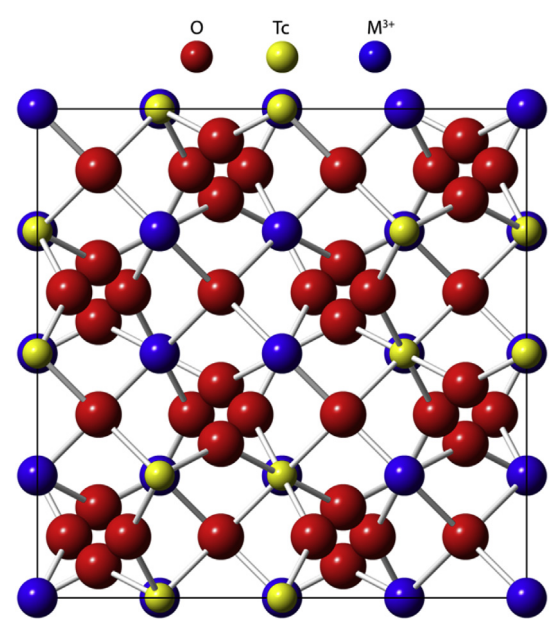

Fig. 7. Model of a pyrochlore unit cell based off of $Dy_2Tc_2O_7$ by Muller et al. [21]. The structure is shown normal to the *a* direction.

propagating, high-temperature synthesis are found to contain the most Mo, followed by perovskite, then pyrochlore.

The high temperatures that these reactions occur at obviously present a challenge to Tc applications because of the volatility of Tc.

2.4. Tin oxide

Sintered SnO_2 doped with Sb^{3+} and Sb^{5+} share the tetragonal space group $P4_2/mnm$ with rutile [115]. This mixed oxide is able to selectively reductively eliminate TcO_4^- out of solutions, reducing it to Tc^{4+} during the process [30]. This is not an ionic exchange; rather, an incorporation of Tc into lattice vacancies occurs even in the presence of competing ions such as Cl^-, NO_3^-, Ca^{2+}, and NH_4^+ [116]. The Tc-doped SnO_2 has been shown to be a suitable host phase for Tc, It has high chemical durability and can be heated in air without loss of Tc [117].

These properties combined indicate that SnO_2 may be a suitable material to remove Tc from the melter off-gas or other waste streams. Achieving both these objectives with one material and without additional chemical separation or processing of Tc would be minimally disruptive to current WTP processes. Further testing of Tc removal into SnO_2 from off-gas simulants and durability in glass melts are needed to more fully evaluate this material as a viable candidate material.

2.5. Pyrochlore

Pyrochlore is from the cubic space group *Fd*-3*m* and has a general formula of either $A_2B_2O_6$ or $A_2B_2O_7$, where the A and B are most often rare earth or transition metals [118]. An example of a pyrochlore structure is presented in Fig. 7. Pyrochlore has been examined as a waste form for actinides, and may be synthesized through diverse routes such as sintering, hydrothermal processes, and ball-milling. As discussed in Laverov et el. [112], self-propagating. high-temperature synthesis can form pyrochlore as a product phase. Pyrochlore also can incorporate technetium, and shows lower leach rates than waste glasses [112]. Several high-temperature syntheses methods have been designed for Tc-bearing pyrochlore.

In a procedure similar to that taken by Muller et al. [21], pyrochlore phases for Tc^{4+} and a number of lanthanides were achieved by sintering oxides in vacuum at 1150 °C [19]. For Pr, Nd, Sm, and Gd unreacted reagents were 1–5%. The particle size was calculated to be 120 nm [20]. Lower temperatures of pyrochlore formation were achieved when TcO_2 and either Bi_2O_3 or PbO were combined in a mortar and pestle in methanol and heated to 700 °C under Ar [4]. The challenges of the aforementioned high-temperature synthesis procedures apply to this approach, namely risk of technetium volatility, the need for pure and reduced reagents, and the engineering demands and modifications to WTP.

Rodriguez [4] used Tc_2O_7 to synthesize $Cd_2Tc_2O_7$. Here, Tc_2O_7 and metallic Cd were sintered under vacuum at 800 °C, giving, to the authors' knowledge, the only reported synthesis of a Tc mixed oxide using Tc^{7+} as a reagent. While using Tc of the same oxidation state as is found in LAW (Tc^{7+}), this method is noted as being dependent on the absence of any water, which would pose limitations if adapted for use in the WTP.

When the $Bi_2Tc_2O_7$ product was combined with Bi_2O_3 and heated to 450 °C under O_2, Bi_3TcO_8 was synthesized. This phase is an analogue to Bi_3ReO_8, which has a melting point of 1473 °C because of the ionic nature and fluorite structure, giving it high lattice energy. According to X-ray absorption near edge structure analysis, both Tc^{4+} and Tc^{7+} were present in Bi_3TcO_8 [4].

Re-bearing pyrochlore can also be synthesized by combining ReO_3 and CdO under vacuum in a fused silica ampoule at 1000 °C [119]. The Re and Cd oxidized, volatilized, and condensed on cooler, upper parts of the ampoule, forming millimeter-sized crystals. It is possible that this process could be extrapolated from Re precursors to Tc precursors.

At much lower temperatures and without Tc, the hydrothermal method used in Zeng et al. [120] offers a more energetically favored route to produce nano-particle pyrochlore. Here, $La(NO_3)_3$ and $SnCl_4$ were dissolved in a high pH aqueous solution. A white precipitate that immediately formed was autoclaved at 200 °C for 12 h, which led to $La_2Sn_2O_7$ nano-cubes of ~60-nm per side. This technique may be an applicable for making Tc-doped pyrochlore at low temperatures.

Fuentes et al. [121] used ball-milling to synthesize a distorted pyrochlore structure from Y_2O_3, Gd_2O_3, Dy_2O_3, and TiO_2. Subsequent heating rearranged the oxygen lattice sufficiently to allow a fully ordered pyrochlore to form, and the temperature needed to induce this rearrangement decreased with increasing mill times (806 °C for 9 h milled, 744 °C for 19 h milled). This is similar to other ball-milling techniques to mechano–chemically combine oxides, followed by heating to further crystalize the material. Particle sizes were several nanometers in diameter. Milling was done in zirconia vessel and with zirconia media, and milling time ranged from 1 to 19 h. Contamination of zircon in samples was ≤4%, and rotational speeds were 350 revolutions per minute.

2.6. Perovskite

Perovskite is a mineral phase of the orthorhombic space group *Pnma* with the formula $A^{2+}B^{4+}O_3$, where A is a 2+ cation and B is a 4+ cation. A model of a perovskite is shown in Fig. 8. In the literature, reports of Tc-containing perovskites are common, and Muller et al. [21] demonstrated $SrTcO_3$ with a very slightly distorted perovskite structure. Since then, other Tc-perovskite structures have been synthesized, many by merely varying stoichiometric ratios in procedures that might otherwise yield spinel or pyrochlore [20,21,113].

One such example is $CaTcO_3$, which is made from high-temperature sintering in Ar at 1150 °C for 4 h [122]. Titanium analogues of Tc-perovskite structures exist, and with other mixed oxides, varying levels of Tc and Ti can be prepared. For example, $SrTi_{0.9}Tc_{0.1}O_3$ was made by pressing oxides and firing at 1250 °C for 24 h [43]. Hartmann et al. [20] synthesized $SrTcO_3$, the Tc end-member, under vacuum at 770 °C for seven days, yielding particle

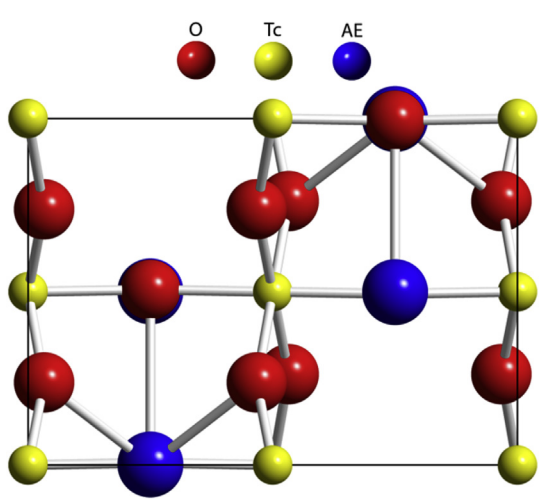

Fig. 8. Model of a $SrTcO_3$ perovskite unit cell after Thorogood et al. [143]. The structure is shown normal to the *c* direction.

sizes of ~120 nm. Then, $CdTcO_3$ was synthesized by grinding TcO_2 and CdO in methanol, followed by heating of this mixture in a fused quartz boat under flowing Ar gas at 850 °C. A similar method was used by Sasaki et al. [123] with high pressures and temperatures to make $CdTiO_3$. Rodriguez [4] used the same approach to synthesize $SrTcO_3$, except that $SrCO_3$ was used instead of the divalent oxide to prevent hygroscopic moistening. As has already been mentioned, self-propagating high temperature synthesis can create particles of perovskite, along with other mixed oxides [112,113].

Rhenium perovskite phases analogous to the Tc species can be formed from ReO_3 and divalent oxides heated to 1000 °C for 24 h in silica crucibles [124]. Cubic phases with the formula $Ba(M_{0.5}Re_{0.5})O_3$ were synthesized, along with distorted $Sr(Fe_{0.5}Re_{0.5})O_3$ and $Ca(Fe_{0.5}Re_{0.5})O_3$. Except in the cases where NiO was a reagent, the products were pure. The phases made were reported to be insoluble in water and HCl, slowly dissolving in nitric acid, and quickly dissolving in hydrogen peroxide.

Another study reports heating these perovskite phases in air to 1000 °C [125], at which point the reagents oxidized and formed $(Ba,Sr)_4Re_2MO_{12}$ (M = Mg, Cd, Co, Zn). The $Sr(Re_{0.5}Ca_{0.5})O_3$ form alone resisted oxidation in air at 1000 °C. There was no discussion of Re volatility, and the given stoichiometry implies that it remained in the new phase when it was formed. With no evidence that Re escaped the perovskite or product structure at 1000 °C, this implies that the volatility usually seen with Re species was inhibited by inclusion in the perovskite, which implies potential usefulness for possible Tc analogues for transporting Tc into the glass during melting.

Other, lower-temperature methods exist to synthesize perovskite. The previously-described sol–gel method was used, starting from metal acetates [72]. Reagents were mineralized with NH_4OH in a sol–gel and then heated to form perovskite. While XRD peaks of the product were detected at 600 °C, the result was not pure perovskite until 1300 °C, a temperature 200 °C lower than conventionally used for sintering. The reaction was complete in hours rather than days. Particle sizes were in the 10-nm range, as verified with TEM [72].

High-temperature sintering can be accomplished at lower temperatures by milling the precursors. Baek et al. [126] used a multi-ring mill that reduced media ablation during use. After milling, the mechano-chemically prepared mixture still required sintering at 850 °C. Crystallinity in samples milled in the ring mill increase to >90% after sintering whereas unmilled samples and ball-milled samples were 8 and 10% crystalline, respectively, after the same heat treatment. This augmented crystallinity was seen across all heat treatments. Using basic metallic hydroxides and acidic metallic oxide pairs in the reagents increased the reactivity of the species and aided in the formation of complex oxide forms. By varying the stoichiometry of the starting reagents, pyrochlore-rich or pyrochlore-free perovskite were produced.

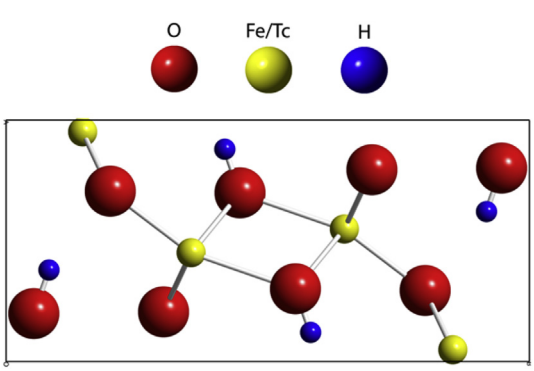

Fig. 9. Model of a FeO(OH) (goethite) unit cell after Yang et al. [128] where Tc can substitute into the structure for Fe^{3+}. The structure is shown normal to the *c* direction.

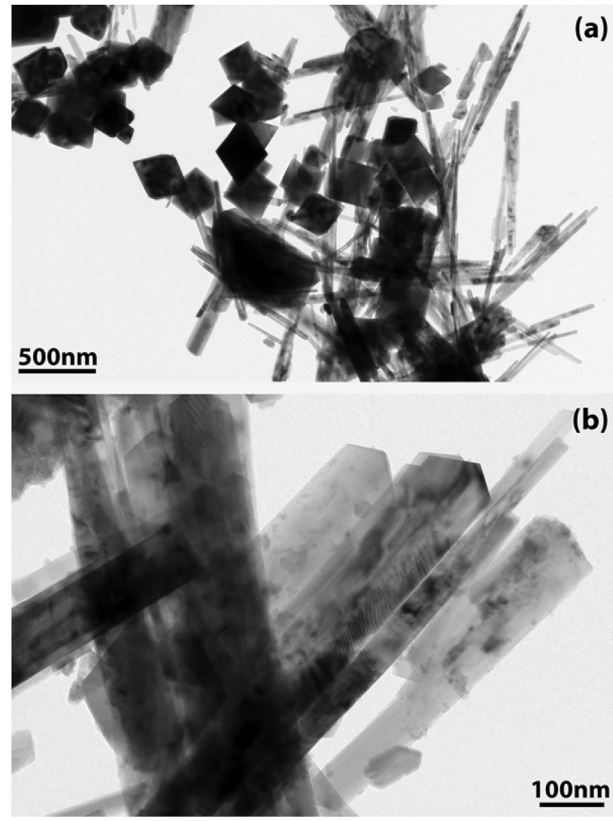

Fig. 10. TEM micrographs of (a) goethite (rods) with magnetite (octahedral) at and (b) goethite [22,23].

Urban et al. [127] synthesized $(Sr,Ba)TiO_3$ nanorods from bimetallic alkoxides and highly oxidizing aqueous solutions. Concentrated H_2O_2 decomposed the organic ligands on the metal at 280 °C and precipitates out the nanorods, which were 60 nm × 10 μm. This approach is a one-step, low temperature synthesis of the perovskite phase, but would be unlikely to capture Tc^{4+} in the Ti sites because of the very oxidizing conditions and the tendency of Tc^{4+} to oxidize to Tc^{7+} under this environment.

2.7. Goethite

Goethite is a mineral of the orthorhombic space group *Pbnm* and has the general formula of AO(OH) where A is one or a mix of metals but the most typical form is FeO(OH) as is shown in Fig. 9 [128]. Goethite has been successfully prepared with Tc by means of an aqueous co-precipitation [22,23] as Fig. 10 illustrates. Divalent iron in solution with Tc^{7+} produced goethite when mineralized at pH > 7. All Tc^{7+} was reduced to Tc^{4+} and was removed from the solution with the Fe^{2+}, which oxidized to Fe^{3+}. When further goethite-forming $Fe(NO_3)_3$ was added to 'armor' the goethite particles, very little Tc re-oxidation was observed in leaching tests. Goethite is one of only two Tc-bearing phases to be doped into LAW feed and melted into glass in crucible tests [129]. Preliminary results indicate that Tc retention was increased relative to tests where $KTcO_4$ was used as a Tc source run in identical conditions.

2.8. Layered double hydroxides

Layered double hydroxides are metal hydroxides arranged in

sheets with hydroxide ions, and have a formula $A^{2+}B^{3+}(OH)_5$. Examples such as fougerite (green rust) [24] and sulfide-based layered double hydroxides such as potassium metal sulfides (KMS-2) [15] have been observed to incorporate Tc. These are proposed as a route to remove Tc from liquid waste streams, and are able to pull Tc out of such solutions, although competition from other anions makes this method problematic [26] and low structural stability makes them less than ideal.

2.9. Magnesium phosphates

Magnesium phosphates, such as ceramicrete and $MgKPO_4$ were proposed as a Tc waste forms [112,130]. Reducing agents in the form of blast furnace slag or $SnCl_2$ stabilize the Tc^{4+} which incorporates into the phosphate [26]. The reaction is exothermic and nearly instantaneous, and forms a monolithic solid with evenly dispersed Tc [131]. Singh et al. [132] formed a Mg-K-PO_4 ceramic by adding a binding mixture ($MgO + KH_2PO_4$) to an aqueous solution of Tc with 1 M NaOH and 1 M ethylenediamine in an anoxic environment. $SnCl_2$ was added as reducing agent, and fly ash was added as a mechanical strengthener.

2.10. Cementitous waste

Cementitous grouts, including saltstone and Cast Stone have been studied as matrices for Tc-containing waste. Saltstone was investigated by Savannah River National Laboratory to immobilize Tc, among other radionuclides in LAW [10]. Salt solutions of LAW are mixed with blast furnace slag, fly ash, and calcium hydroxide in a wide range of ratios to form cement. The cements were cured in water for several weeks. When $SnCl_2$ is added as a reducing agent, the leaching rate of Tc from these matrices is lowered [15]. Portland cement, fly ash, and blast furnace slag mixed in different amounts were shown to effect performance, with fly ash promoting Tc reduction into Tc^{4+} and lowering leach rates by several orders of magnitude [9]. Other Tc getters can be added to LAW solutions to pull Tc from solution, then kept in the waste during the cement-forming process [15]. A major drawback to cementitious waste forms is the vulnerability to re-oxidation. Lukens [133] showed that, while Tc remained as Tc^{4+} when cement was under anoxic conditions, after exposure to air, it reoxidized to Tc^{7+}. This vulnerability to re-oxidation makes cement a poor candidate to transport Tc^{4+} across the cold-cap and into glass melts.

2.11. Metal alloys

Metallic Tc can be transmuted into Ru to a limited extent, or made into chemically durable waste forms [8]. Metallic Tc forms alloys with Fe, Zr, Mo, Pd, Rh, Ru, and actinides [134,135]. The ε-metal is an alloy of Tc, Mo, Pd, Rh, and Ru formed in nuclear fuel rods and in natural uranium fission [136]. Stainless steel alloys containing Zr have been made from spent fuel cladding hardware and noble metals from dissolved spent nuclear fuel where the Tc loading is around ~2 mass% and the Tc partitions into the ferrite and austenite phases rather than the Zr-based intermetallic phases [137,138]. Methods for synthesizing Tc alloys include furnace melting, molten salt methods, arc melting, and hot pressing techniques (e.g., hot isostatic pressing, spark plasma sintering, and microwave sintering) [26,27].

Additionally, direct electrolytic reduction of TcO_4^- from solutions to Tc metal such as off-gas scrubber streams has been shown to be unsatisfactory, yielding incomplete reduction and Tc^{4+} species [139], but has been demonstrated with some success on Hanford tank waste [140].

3. Summary

Technetium can be incorporated into a number of different solids including spinel, sodalite, rutile, tin dioxide, pyrochlore, perovskite, goethite, layered double hydroxides, cements, and alloys. Synthesis routes are possible for each of these phases, ranging from high-temperature ceramic sintering to ball-milling of constituent oxides. However, in practice, Tc has only been incorporated into solid materials by a limited number of the possible syntheses approaches.

In this document, we provided a review of the diverse ways in which Tc-immobilizing materials can be made, showing the range of options available. In some cases, synthesis of the solids has been demonstrated in the literature with Tc; however, in other cases, it has not been demonstrated but likely could be synthesized using one or more of the techniques provided. The primary aim of this document is to provide a summary of the current state-of-the-art in making Tc-containing materials and materials that could act as a host for Tc.

Acknowledgments

This work was supported by the U.S. Department of Energy's Waste Treatment and Immobilization Plant Federal Project Office under the direction of Dr. Albert A. Kruger. Pacific Northwest National Laboratory is operated for the Department of Energy by Battelle Memorial Institute under contract DE-AC05-76RL01830. The authors would like to Dong-Sang Kim, Chuck Soderquist, Derek Dixon, and Wooyong Um for their guidance during this work.

References

[1] P. Certa, P. Empey, M. Wells, River Protection Project System Plan, ORP-11242, Rev. 6, DOE Office of River Protection, Richland, WA, 2011.
[2] V. Neck, B. Kanellakopulos, Radiochim. Acta 42 (3) (1987) 135–137.
[3] K. Morris, F.R. Livens, J.M. Charnock, I.T. Burke, J.M. McBeth, J.D.C. Begg, C. Boothman, J.R. Lloyd, Appl. Geochem. 23 (4) (2008) 603–617.
[4] E.E. Rodriguez, Solid State Chemistry of Technetium and Rhenium Oxides, Ph.D. thesis, University of California, Santa Barbara, 2009.
[5] J. Gibson, Radiochim. Acta 60 (2–3) (1993) 121–126.
[6] J.G. Darab, P.A. Smith, Chem. Mater. 8 (5) (1996) 1004–1021.
[7] Y. Olsen, J.V. i Batlle, J. Environ. Radioact. 67 (3) (2003) 219–233.
[8] J. Bonnerot, V. Broudic, M. Phelip, C. Jégou, F. Varaine, X. Deschanels, M. Arnoux, J. Faugèrea, J. Nucl. Radiochem. Sci. 6 (3) (2005) 287–290.
[9] T.M. Gilliam, R.D. Spence, W.D. Bostick, J. Shoemaker, J. Hazard. Mater. 24 (2) (1990) 189–197.
[10] C. Langton, E. Wilhite, Proc. INEt (1988) 56.
[11] R.J. Serne, J.H. Westsik, Data Package for Secondary Waste Form Down-selection—cast Stone, PNNL-20706, Pacific Northwest National Laboratory, Richland, WA, 2011.
[12] D. Missimer, R. Rutherford, Preparation and Initial Characterization of Fluidized Bed Steam Reforming Pure-phase Standards, SRNL-STI-2013-00111, Savannah River National Laboratory, Aiken, SC, 2013.
[13] S.V. Mattigod, R.J. Serne, G.E. Fryxell, Selection and Testing of "Getters" for Adsorption of Iodine-129 and Technetium-99: a Review, PNNL-14208, Pacific Northwest National Laboratory, Richland, WA, Richland, WA, 2003.
[14] M. Morse, C. Nash, Experimental Ion Exchange Column with SuperLig 639 and Simulant Formulation, SRNL-L3100-2013-00157, Savannah River Site, Aiken, SC, 2013.
[15] N.P. Qafoku, J.J. Neeway, A.R. Lawter, T.G. Levitskaia, R.J. Serne, J.J. Westsik, M.M.V. Snyder, Technetium and Iodine Getters to Improve Cast Stone Performance, PNNL-23282, Pacific Northwest National Laboratory, Richland, WA, 2014.
[16] S.A. Luksic, B.J. Riley, D.-S. Kim, P. Hrma, M.J. Schweiger, W. Um, C.I. Pearce, C.Z. Soderquist, Use of Mineral Phases to Increase Re and Tc Retention in Waste Glass Simulants (in press), Pacific Northwest National Laboratory, Richland, WA, 2015.
[17] B. Kenna, P. Kuroda, J. Inorg. Nucl. Chem. 26 (4) (1964) 493–499.
[18] M.J. den Exter, S. Neumann, T. Tomasberger, in: P. Van Iseghem (Ed.), In the Proc.. of Sci. Basis Nucl. Waste Manag., Materials Research Society, 2006, pp. 567–574. XXIX 932.
[19] T. Hartmann, A. Alaniz, F. Poineau, P. Weck, J. Valdez, M. Tang, G. Jarvinen, K. Czerwinski, K. Sickafus, J. Nucl. Mater. 411 (1) (2011) 60–71.
[20] T. Hartmann, A.J. Alaniz, D.J. Antonio, Procedia Chem. 7 (2012) 622–628.
[21] O. Muller, W.B. White, R. Roy, J. Inorg. Nucl. Chem. 26 (12) (1964)

2075–2086.
[22] W. Um, H.-s. Chang, J.P. Icenhower, W.W. Lukens, R.J. Serne, N.P. Qafoku, J.J. Westsik, E.C. Buck, S.C. Smith, Environ. Sci. Technol. 45 (11) (2011), 4904–1913.
[23] W. Um, H.-s. Chang, J.P. Icenhower, N. Qafoku, S.C. Smith, R.J. Serne, E.C. Buck, R.K. Kukkadapu, M.E. Bowden, J.H. Westsik, Immobilization and Limited Reoxidation of Technetium-99 by Fe (II)-goethite, Pacific Northwest National Laboratory, Richland, WA, 2010. PNNL-19833.
[24] I. Alliot Llorens, P. Deniard, E. Gautron, A. Olicard, M. Fattahi, S. Jobic, B. Grambow, Radiochim. Acta 96 (9–11) (2008) 569–574.
[25] M. Kang, S. Rhee, H. Moon, V. Neck, T. Fanghanel, Radiochim. Acta 75 (3) (1996) 169–173.
[26] J.J. Westsik, K. Cantrell, R. Serne, N. Qafoku, Technetium Immobilization Forms Literature Survey, PNNL-23329, EMSP-RPT-023, Pacific Northwest National Laboratory, Richland, WA, 2014.
[27] J.V. Crum, D. Strachan, A. Rohatgi, M. Zumhoff, J. Nucl. Mater. 441 (1–3) (2013) 103–112.
[28] W.W. Lukens, N. Magnani, T. Tyliszczak, D.K. Shuh, In Proc.. of the American Chemical Society, 2012 (DOE BES CSGB Review).
[29] S.V. Mattigod, B. Peter McGrail, D.E. McCready, L.-Q. Wang, K.E. Parker, J.S. Young, Micropor. Mesopor. Mater. 91 (1–3) (2006) 139–144.
[30] R. Koivula, Cent. Eur. J. Chem. 8 (6) (2010) 1179–1184.
[31] I.L. Pegg, J. Radioanal. Nucl. Chem. 305 (1) (2015) 287–292.
[32] W.W. Lukens, D.K. Shuh, N.C. Schroeder, K.R. Ashley, 38(1) (2004) 229–233.
[33] J. Liu, C.I. Pearce, O. Qafoku, E. Arenholz, S.M. Heald, K.M. Rosso, 92 (2012) 67–81.
[34] J.K. Burdett, G.D. Price, S.L. Price, J. Am. Chem. Soc. 104 (1) (1982) 92–95.
[35] C.M.B. Henderson, J.M. Charnock, D.A. Plant, J. Phys.-Condens. Mat. 19 (7) (2007) 076214.
[36] T.A. Marshall, K. Morris, G.T.W. Law, J.F.W. Mosselmans, P. Bots, S.A. Parry, S. Shaw, Environ. Sci. Technol. 48 (20) (2014) 11853–11862.
[37] C.I. Pearce, C.M.B. Henderson, N.D. Telling, R.A.D. Pattrick, J.M. Charnock, V.S. Coker, E. Arenholz, F. Tuna, G. van der Laan, Am. Mineral. 95 (2010) 425–439.
[38] S.W.A. Bligh, P.J. Sadler, J.A. Marriott, I.A. Latham, J.D. Kelly, Int. J. Radiat. Appl. Instrum. Part A 40 (9) (1989) 751–757.
[39] U. Colombo, F. Gazzarrini, G. Lanzavecchia, G. Sironi, Science 147 (3661) (1965) 1033.
[40] S. Laurent, D. Forge, M. Port, A. Roch, C. Robic, L. Vander Elst, R.N. Muller, Chem. Rev. 108 (6) (2008) 2064–2110.
[41] F.N. Skomurski, K.M. Rosso, K.M. Krupka, B.P. McGrail, Environ. Sci. Technol. 44 (15) (2010) 5855–5861.
[42] W.J. Deutsch, K.J. Cantrell, K.M. Krupka, M.L. Lindberg, R. Jeffery Serne, Appl. Geochem. 26 (9–10) (2011) 1681–1693.
[43] M.Y. Khalil, W.B. White, in: G.L. McVay (Ed.), In the Proc. of Sci. Basis Nucl. Waste Manag., Elsevier, 1984, pp. 655–662. VII 26.
[44] G.J. Thorogood, Z. Zhang, J.R. Hester, B.J. Kennedy, J. Ting, C.J. Glover, B. Johannessen, Dalton Trans. 40 (41) (2011) 10924–10926.
[45] W. Um, S. Luksic, G. Wang, D.-S. Kim, M. Schweiger, P. Hrma, A. Kruger (in press), Proc. Waste Manag. (2015).
[46] D. Chen, D. Chen, X. Jiao, Y. Zhao, M. He, Powder Technol. 133 (1) (2003) 247–250.
[47] S.A. Luksic, B.J. Riley, Molten Salt Synthesis of Spinel, Pacific Northwest National Laboratory, Richland, WA, 2015 (in press).
[48] P. Laokul, V. Amornkitbamrung, S. Seraphin, S. Maensiri, Curr. Appl. Phys. 11 (1) (2011) 101–108.
[49] S. Bid, P. Sahu, S. Pradhan, Phys. E 39 (2) (2007) 175–184.
[50] J. Calbo, M. Tena, G. Monrós, M. Llusar, J. Badenes, J. Sol-Gel Sci. Technol. 38 (2) (2006) 167–177.
[51] M.Y. Khalil, W.B. White, J. Am. Ceram. Soc. 66 (10) (1983) c197–c198.
[52] H.T. Kim, Y. Kim, M. Valant, D. Suvorov, J. Am. Ceram. Soc. 84 (5) (2001) 1081–1086.
[53] E.E. Rodriguez, F. Poineau, A. Llobet, A.P. Sattelberger, J. Bhattacharjee, U.V. Waghmare, T. Hartmann, A.K. Cheetham, J. Am. Chem. Soc. 129 (33) (2007) 10244–10248.
[54] K. Righter, Proc. Lunar Planet. Inst. Sci. Conf. Abstr. 32 (2001) 1759.
[55] S.B. Shirey, R.J. Walker, Anal. Chem. 67 (13) (1995) 2136–2141.
[56] J. Chen, C. Sorensen, K. Klabunde, G. Hadjipanayis, E. Devlin, A. Kostikas, Phys. Rev. B 54 (13) (1996) 9288–9296.
[57] C.I. Pearce, O. Qafoku, J. Liu, E. Arenholz, S.M. Heald, R.K. Kukkadapu, C.A. Gorski, C.M.B. Henderson, K.M. Rosso, J. Colloid Interface Sci. 387 (1) (2012) 24–38.
[58] C.R. Vestal, Z.J. Zhang, Nano Lett. 3 (12) (2003) 1739–1743.
[59] C. Liu, B. Zou, A.J. Rondinone, Z.J. Zhang, J. Phys. Chem. B 104 (6) (2000) 1141–1145.
[60] O. Perales-Perez, Y. Umetsu, Hydrometallurgy 55 (1) (2000) 35–56.
[61] N. Gribanov, E. Bibik, O. Buzunov, V. Naumov, J. Magn. Magn. Mater. 85 (1) (1990) 7–10.
[62] M. Hirano, S. Okumura, Y. Hasegawa, M. Inagaki, J. Solid State Chem. 168 (1) (2002) 5–10.
[63] Y.-I. Jang, H. Wang, Y.-M. Chiang, J. Mater. Chem. 8 (12) (1998) 2761–2764.
[64] G. Gnanaprakash, S. Mahadevan, T. Jayakumar, P. Kalyanasundaram, J. Philip, B. Raj, Mater. Chem. Phys. 103 (1) (2007) 168–175.
[65] A.S. Albuquerque, J.D. Ardisson, W.A. Macedo, M. Alves, J. Appl. Phys. 87 (9) (2000) 4352–4357.
[66] B. Domenichini, D. Aymes, P. Perriat, B. Gillot, Mater. Chem. Phys. 39 (1) (1994) 80–84.
[67] I. Martínez-Mera, M. Espinosa-Pesqueira, R. Pérez-Hernández, J. Arenas-Alatorre, Mater. Lett. 61 (23) (2007) 4447–4451.
[68] D. Gherca, A. Pui, N. Cornei, A. Cojocariu, V. Nica, O. Caltun, J. Magn. Magn. Mater. 324 (22) (2012) 3906–3911.
[69] P. Poddar, H. Srikanth, S. Morrison, E. Carpenter, J. Magn. Magn. Mater. 288 (2005) 443–451.
[70] C. Liu, A.J. Rondinone, Z.J. Zhang, Pure Appl. Chem. 72 (1) (2000) 37–45.
[71] T. Giannakopoulou, L. Kompotiatis, A. Kontogeorgakos, G. Kordas, J. Magn. Magn. Mater. 246 (3) (2002) 360–365.
[72] K. Huang, M. Feng, J.B. Goodenough, J. Am. Ceram. Soc. 79 (4) (1996) 1100–1104.
[73] Q. Song, Z.J. Zhang, J. Am. Chem. Soc. 126 (19) (2004) 6164–6168.
[74] Q. Song, Y. Ding, Z.L. Wang, Z.J. Zhang, Chem. Mater. 19 (19) (2007) 4633–4638.
[75] Q. Song, Z.J. Zhang, J. Am. Chem. Soc. 134 (24) (2012) 10182–10190.
[76] L. Pérez-Mirabet, E. Solano, F. Martínez-Julián, R. Guzmán, J. Arbiol, T. Puig, X. Obradors, A. Pomar, R. Yáñez, J. Ros, Mater. Res. Bull. 48 (3) (2013) 966–972.
[77] J.-F. Pasquier, S. Komarneni, R. Roy, J. Mater. Sci. 26 (14) (1991) 3797–3802.
[78] V. Kuznetsova, O. Almjasheva, V. Gusarov, Glass Phys. Chem. 35 (2) (2009) 205–209.
[79] M. Sisk, I. Kilbride, A. Barker, J. Mater. Sci. Lett. 14 (3) (1995) 153–154.
[80] J. Zhang, J. Shi, M. Gong, J. Solid State Chem. 182 (8) (2009) 2135–2140.
[81] Z. Xing, Z. Ju, J. Yang, H. Xu, Y. Qian, Nano Res. 5 (7) (2012) 477–485.
[82] A.R. Gainsford, M.J. Sisley, T.W. Swaddle, P. Bayliss, Can. J. Chem. 53 (1) (1975) 12–19.
[83] A. Alarifi, N. Deraz, S. Shaban, J. Alloys Compd. 486 (1–2) (2009) 501–506.
[84] M.J. Geselbracht, L.D. Noailles, L.T. Ngo, J.H. Pikul, R.I. Walton, E.S. Cowell, F. Millange, D. O'Hare, Chem. Mater. 16 (6) (2004) 1153–1159.
[85] T. Kimura, Molten Salt Synthesis of Ceramic Powders, in: C. Sikalidis (Ed.), In Advances in Ceramics - Synthesis and Characterization, Processing and Specific Applications, InTech, 2011.
[86] P. Afanasiev, C. Geantet, Coord. Chem. Rev. 178 (2) (1998) 1725–1752.
[87] B. Senthilkumar, R. Kalai Selvan, P. Vinothbabu, I. Perelshtein, A. Gedanken, Mater. Chem. Phys. 130 (1) (2011) 285–292.
[88] S. Ziemniak, A. Gaddipati, P. Sander, S. Rice, J. Phys. Chem. Solids 68 (8) (2007) 1476–1490.
[89] S.L. Darshane, S. Suryavanshi, I. Mulla, Ceram. Int. 35 (5) (2009) 1793–1797.
[90] S. Zhang, J. Pak, Mater. Soc. 1 (2) (2007) 49–53.
[91] Y. Hayashi, T. Kimura, T. Yamaguchi, J. Mater. Sci. 21 (8) (1986) 2876–2880.
[92] D. Su, M. Ford, G. Wang, Sci. Rep. 2 (924) (2012) 1–7.
[93] Č. Jovalekić, M. Zdujić, A. Radaković, M. Mitrić, Mater. Lett. 24 (6) (1995) 365–368.
[94] M. Zdujić, O. Milošević, L.Č. Karanović, Mater. Lett. 13 (2) (1992) 125–129.
[95] D. Domanski, G. Urretavizcaya, F.J. Castro, F.C. Gennari, J. Am. Ceram. Soc. 87 (11) (2004) 2020–2024.
[96] E. Yalamaç, S. Akkurt, M. Çiftçioğlu, Key Eng. Mater. 264 (2004) 53–56.
[97] C. Henderson, D. Taylor, Spectrochim. Acta, Part A 33 (3) (1977) 283–290.
[98] M. Fechtelkord, Solid State Nucl. Magn. Reson. 18 (1) (2000) 70–88.
[99] J.O. Dickson, J.B. Harsh, M. Flury, W.W. Lukens, E.M. Pierce, Environ. Sci. Technol. 48 (21) (2014) 12851–12857.
[100] W.C. Lepry, B.J. Riley, J.V. Crum, C.P. Rodriguez, D.A. Pierce, J. Nucl. Mater. 442 (1) (2013) 350–359.
[101] I. Hassan, D. Grundy, Can. Mineral. 27 (1989) 165–172.
[102] L. Heller-Kallai, I. Lapides, Appl. Clay Sci. 35 (1) (2007) 99–107.
[103] B. Marinder, A. Magneli, Acta Chem. Scand. 12 (1958) 1153–1158.
[104] M. Stewart, E. Vance, R. Day, WM-4362, in: In the Proc. of Proc. Waste Manage. Symp., 2004.
[105] Y. Iida, S. Ozaki, J. Am. Ceram. Soc. 44 (3) (1961) 120–127.
[106] E.F. Heald, C.W. Weiss, Am. Mineral. 57 (1–2) (1972) 10–23.
[107] K. MacKenzie, Trans. J. Br. Ceram. Soc. 74 (2) (1975) 29–34.
[108] K. Mackenzie, Trans. J. Br. Ceram. Soc. 74 (3) (1975) 77–84.
[109] K. MacKenzie, Trans. J. Br. Ceram. Soc. 74 (4) (1975) 121–125.
[110] K. MacKenzie, Trans. J. Br. Ceram. Soc. 74 (4) (1975) 127–134.
[111] Y. Fu, Z. Jin, Y. Ni, H. Du, T. Wang, Thin Solid Films 517 (19) (2009) 5634–5640.
[112] N. Laverov, S. Yudintsev, B. Omel'yanenko, Geol. Ore Deposits 51 (4) (2009) 259–274.
[113] N. Laverov, S. Yudintsev, E. Konovalov, T. Mishevets, B. Nikonov, B. Omel'yanenko, Dokl. Chem. 431 (1) (2010) 71–75.
[114] N. Laverov, S. Yudintsev, T. Livshits, S. Stefanovsky, A. Lukinykh, R. Ewing, Geochem. Int. 48 (1) (2010) 1–14.
[115] J. Rockenberger, U. Zum Felde, M. Tischer, L. Tröger, M. Haase, H. Weller, J. Chem. Phys. 112 (9) (2000) 4296–4304.
[116] R. Koivula, R. Harjula, Sep. Sci. Technol. 46 (2) (2010) 315–320.
[117] Y.I. Korneyko, in: K.E. German, B.F. Myasoedov, G.E. Kodina, I.D. Troshkina, T. Sekine (Eds.), In the Proc. of 7th International Symposium on Technetium and Rhenium, vol. 44, Granitsa Publishing House, 2011.
[118] H. Nyman, S. Andersson, B. Hyde, M. O'Keeffe, J. Solid State Chem. 26 (2) (1978) 123–131.
[119] P.C. Donohue, J.M. Longo, R.D. Rosenstein, L. Katz, Inorg. Chem. 4 (8) (1965) 1152–1153.
[120] J. Zeng, H. Wang, Y. Zhang, M.K. Zhu, H. Yan, J. Phys. Chem. C 111 (32) (2007)

11879–11887.
[121] A.F. Fuentes, K. Boulahya, M. Maczka, J. Hanuza, U. Amador, Solid State Sci. 7 (4) (2005) 343–353.
[122] M. Avdeev, G.J. Thorogood, M.L. Carter, B.J. Kennedy, J. Ting, D.J. Singh, K.S. Wallwork, J. Am. Chem. Soc. 133 (6) (2011) 1654–1657.
[123] S. Sasaki, C.T. Prewitt, J.D. Bass, W. Schulze, Acta Cryst. C 43 (9) (1987) 1668–1674.
[124] J. Longo, R. Ward, J. Am. Chem. Soc. 83 (13) (1961) 2816–2818.
[125] J.M. Longo, L. Katz, R. Ward, Inorg. Chem. 4 (2) (1965) 235–241.
[126] J.G. Baek, T. Isobe, M. Senna, J. Am. Ceram. Soc. 80 (4) (1997) 973–981.
[127] J.J. Urban, W.S. Yun, Q. Gu, H. Park, J. Am. Chem. Soc. 124 (7) (2002) 1186–1187.
[128] H.X. Yang, R. Lu, R.T. Downs, G. Costin, Acta Cryst. E. 62 (2006) i250–i252.
[129] W. Um, S.A. Luksic, P. Hrma, Proc. Waste Manag (2015) (in press).
[130] A. Wagh, M. Maloney, G. Thomson, A. Antink, 3 (2003).
[131] S. Vinokurov, Y.M. Kulyako, O. Slyuntchev, S. Rovny, B. Myasoedov, J. Nucl. Mater. 385 (1) (2009) 189–192.
[132] D. Singh, V. Mandalika, S. Parulekar, A. Wagh, J. Nucl. Mater. 348 (3) (2006) 272–282.
[133] W.W. Lukens, J.J. Bucher, D.K. Shuh, N.M. Edelstein, Environ. Sci. Technol. 39 (20) (2005) 8064–8070.
[134] J.V. Crum, D. Strachan, A. Rohatgi, M. Zumhoff, 441(1) (2013) 103–112.
[135] C.D. Taylor, J. Metall. 2011 (2011) 1–8.
[136] S. Utsunomiya, R.C. Ewing, Radiochim. Acta 94 (9–11) (2006) 749–753.
[137] D.D. Keiser Jr., D.P. Abraham, J.W. Richardson Jr., J. Nucl. Mater. 277 (2–3) (2000) 333–338.
[138] S.M. McDeavitt, D.P. Abraham, J.Y. Park, J. Nucl. Mater 257 (1) (1998) 21–34.
[139] J. Eakins, D. Humphries, J. Inorg. Nucl. Chem. 25 (6) (1963) 737.
[140] W.E. Lawrence, D.L.J. Blanchard, D.E. Kurath, Electrochemical Reduction Removal of Technetium-99 from Hanford Tank Wastes, PNNL-11696, Pacific Northwest National Laboratory, Richland, WA, 1997.
[141] F. Bosi, U. Hålenius, H. Skogby, Am. Mineral. 94 (1) (2009) 181–189.
[142] C.M.B. Henderson, K.S. Neuhoff, A.R. Lennie, Open Mineral. J. 3 (2009) 1–11.
[143] G.J. Thorogood, M. Avdeev, M.L. Carter, B.J. Kennedy, J. Ting, K.S. Wallwork, Dalton Trans. 40 (27) (2011) 7228–7233.